Int J Clin Exp Pathol 2020;13(2):192-202
www.ijcep.com /ISSN:1936-2625/IJCEP0105453

Original Article

Kidney and lung tissue modifications after BDL-induced liver injury in mice are associated with increased expression of IGFBPrP1 and activation of the NF-κB inflammation pathway

Zhi-Hui Hu[1], Yang-Yang Kong[1], Jun-Jie Ren[1], Ting-Juan Huang[1], Yan-Qin Wang[1], Li-Xin Liu[1,2,3]

[1]Department of Gastroenterology and Hepatology, [2]Experimental Center of Science and Research, The First Hospital of Shanxi Medical University, Taiyuan 030001, China; [3]Key Laboratory of Cell Physiology, Department of The Ministry of Education, Shanxi Medical University, Taiyuan 030001, China

Received November 25, 2019; Accepted January 23, 2020; Epub February 1, 2020; Published February 15, 2020

Abstract: Background: Hepatorenal and hepatopulmonary syndrome are common clinical diseases; however, their mechanisms have not been fully elucidated. Our aim was to determine whether liver injury by bile duct ligation (BDL) causes modifications in kidney and lung tissue in mice, and to explore the possible mechanism of these changes. Methods: BDL in mice was used as a research model. Pathologic changes of liver, kidney, and lung tissue were observed by hematoxylin-eosin (H&E) staining. The expression of IGFBPrP1, NF-κB, TNF-α, and IL-6 were investigated in liver, kidney, and lung tissue by immunohistochemical staining and western blot. The correlation between IGFBPrP1 and NF-κB, TNF-α, and IL-6 protein expression in liver, kidney, and lung tissues of each group was analyzed by the Pearson method. Results: H&E staining showed, after BDL administration in mice, different degrees of inflammatory change in liver, kidney, and lung tissues of mice in each group. The results of immunohistochemical staining and western blot analysis showed increased expressions of IGFBPrP1, NF-κB, TNF-α, and IL-6 after BDL. Pearson correlation analysis showed that IGFBPrP1 positively correlated with the expressions of NF-κB, TNF-α, and IL-6. Conclusion: Liver injury caused by bile duct ligation can lead to kidney and lung tissue injury in mice. The mechanism of injury may be related to the high expression of liver injury factor IGFBPrP1, transcription factor NF-κB, proinflammatory cytokine TNF-α, and IL-6 in kidney and lung tissue. Moreover, an increased expression level of IGFBPrP1 may be accompanied by the activation of the NF-κB inflammatory pathway.

Keywords: Bile duct ligation, insulin-like growth factor binding protein related protein 1, nuclear factor-κB, mouse, kidney, lung

Introduction

Cholestasis caused by stones, inflammation, and tumors of the biliary tract system are a common clinical problem. When cholestasis occurs, a large amount of bile accumulates in the liver and destroys the structure of the biliary tract. The bile enters the blood, causing serious damage to the body. The liver becomes the first damaged organ. Inflammatory cell infiltration, fibroblast proliferation, and hepatocyte degeneration and necrosis in liver tissue lead to cholestasis of hepatic fibrosis and cirrhosis, and may further develop into hepatopulmonary syndrome, hepatorenal syndrome, and multiple organ failure [1, 2]. The multiple organ (liver, kidney and lung) dysfunction caused by cholestasis, has a high incidence rate, high mortality, is expensive to treat, and threatens lives [3, 4]. Therefore, it is of clinical significance to study the mechanism of multiple organ damage caused by cholestasis.

Activation of the inflammatory response involves many pro-inflammatory cytokines such as tumor necrosis factor (TNF)-α, interleukin (IL)-6, IL-β, IL-10, and other inflammatory mediators. Overexpression of these inflammatory mediators can lead to a variety of adverse reactions. TNF-α, which acts as a first-line cytokine, plays a very important role. It is produced by mononuclear macrophages, has functions of

immune regulation, and participates in fever and inflammation. IL-6 is a cytokine that is a sensitive index reflecting the severity of inflammation and tissue injury. Its elevation can exacerbate oxidative stress and lead to the release of toxic metabolites, which causes tissue injury [5, 6]. Moreover, IL-6 can be induced by TNF-α. Nuclear factor (NF)-κB is a transcription factor that plays a key role in the expression of pro-inflammatory cytokine genes [7]. At rest, NF-κB is a heterodimer composed of p65 and p50 (p65/p50) and its endogenous inhibitor of NF-κB (I-κB) binds to the cytoplasm and is regulated by cytokines. When stimulated by various damage factors such as lipopolysaccharides, I-κB degrades, releasing the NF-κB subunit that enters the nucleus to bind to the corresponding target gene, enhancing transcriptional activity, and regulating pro-inflammatory cytokines TNF-α, and IL-6. Other inflammatory mediators are also produced and in large quantities, triggering an inflammatory response. Therefore, detecting the expression of the p65 subunit in the nucleus can indirectly reflect the activation of NF-κB and the degree of inflammatory response.

Insulin-like growth factor binding protein related protein 1 (IGFBPrP1) is a secreted protein that can independently participate in a variety of biologic functions. Our previous study found that IGFBPrP1 can promote the activation of hepatic stellate cells (HSCs) in mice with bile duct ligation [8], produce excessive extracellular matrices, and promote the development of liver fibrosis [9]. Moreover, it could enhance the DNA binding activity of NF-κB p65 in the HSC [10]. In addition, adenovirus carrying IGFBPrP1 can induce kidney and lung tissue injury in Sprague Dawley (SD) rats to varying degrees. The presence or absence of kidney and lung tissue damage, after hepatic injury induced by bile duct ligation in mice is yet to be determined. If this injury does exist, its relation to the pro-inflammatory cytokine TNF-α, to IL-6 which responds to tissue damage, and to the regulation of transcriptional activation of NF-κB, and the liver injury factor IGFBPrP1 has not yet been reported.

A large number of studies have shown that cholestatic cirrhosis can be simulated by performing bile duct ligation (BDL) surgery on mice. This model is ideal for studying the pathogenesis of cholestasis, since it closely mimics human cholestasis liver fibrosis. It is also similar to the histologic changes of human small nodular cirrhosis. Consequently, as a research model, we will use bile duct ligation in mice to determine if there is damage to kidney and lung tissues after liver injury. We will also explore whether this damage is related to pro-inflammatory cytokine TNF-α, or IL-6 which responds to tissue damage, the regulation of transcriptional activation of NF-κB and liver injury factor IGFBPrP1; and the relationship between the four. This study aims to provide new ideas for elucidating the pathogenesis of hepatorenal and hepatopulmonary syndrome.

Materials and methods

Animal models

A total of 78 clean grade C57BL/6 wild type male mice, approximately 3-4 weeks old with a body weight of 18±2 g, were used in this study. These mice were provided by the Institute of Experimental Animals, Academy of Military Medical Sciences (Beijing, China), with animal license number SCXK (Beijing) 2014-0013. The animal study protocol was in compliance with the guidelines of China for animal care, and confor to the internationally accepted principles for care and use of experimental animals.

All animals were kept in the animal room of the Department of Pharmacology, Shanxi Medical University. The indoor temperature was 23±2°C, with a 12 h light-dark cycle, relative humidity of 50±10%. Mice were free to eat specific-pathogen-free (SPF) large mouse growth and breeding feed (Beijing Keao Xieli Feed Co., Ltd.) and had access to drinking water. Experimental work was performed on all animals after one week of adaptive feeding.

Animal grouping and disposal methods

The 78 mice were randomly divided as follows: 24 in the normal control group (normal group), 24 in the sham operation group (sham group) and 30 in the BDL group. The bile duct was isolated and ligated in the BDL group, and isolated but not ligated in the sham group, while the normal group did not undergo any treatment.

Experimental methods

The body weight of each group of mice was recorded daily and the status was observed. At

the end of 2, 4 and 6 weeks, eight animals in each group were anesthetized by intraperitoneal injection of 4% chloral hydrate. Liver, kidney and lung tissues were removed by laparotomy. Some were fixed with 10% formaldehyde solution, embedded in paraffin, and sectioned for H&E and immunohistochemical staining. The rest of liver, kidney and lung tissues were frozen in liquid nitrogen for 2 h and subsequently frozen at -80°C for western blot analysis.

Hematoxylin-eosin (H&E) staining

The liver, kidney and lung tissue sections of mice were routinely dewaxed, hydrated, stained with hematoxylin-eosin and dried with neutral gum. Thereafter, the pathological changes of each tissue were observed under light microscopy.

Immunohistochemical staining

The distribution and expression of IGFBPrP1, NF-κB, TNF-α, and IL-6 in liver, kidney and lung tissues of each group were observed by immunohistochemical staining. Liver, kidney, and lung tissue sections were routinely dewaxed, hydrated, and incubated with 3% H_2O_2 for 15 min to inactivate endogenous peroxidase. After high-pressure heat repair with citrate buffer, the corresponding primary antibodies, IGFBPrP1 (Abcam), TNF-α (Abcam), IL-6 (Abcam), and NF-κB (Protein-tech), were added and incubated for 1 h at 37°C. Thereafter, a biotinylated secondary antibody was added and incubated for 20 min at 37°C. Finally, staining was detected using DAB (Beyotime). Each stain was replaced with phosphate buffered saline (PBS) as a negative control instead of the primary antibody. Brown or yellow granules were positively expressed in each tissue. The images were semi-quantitatively analyzed using the Image-Pro Plus 6.0 automatic medical image color analysis system. Five fields were randomly selected for each slice to analyze the integral optical density (IOD) value of the brown and tan positive expression sites in the tissues. The higher the IOD value, the stronger the positive expression.

Western blot analysis

The liver, kidney, and lung tissues were stored in a biofreezer at -80°C. Protein from tissue was extracted according to the operation instructions of the KGI whole protein extraction kit. The protein concentration was determined by the BCA method. Sodium dodecyl sulfate-polyacrylamide gel electrophoresis (SDS-PAGE) was performed and the gels were transferred to polyvinylidene fluoride (PVDF) membranes. The membranes were blocked with tris-buffered saline containing Tween 20 (TBST) and 5% skim milk powder at 23°C. Thereafter, the membranes were incubated with primary antibodies for IGFBPrP1 (Abcam), TNF-α (Abcam), IL-6 (Abcam), NF-κB (Protein-tech) and β-actin (Abcam) at 4°C overnight. Horseradish peroxidase (HRP)-labeled secondary antibody was added thereafter. The ECL chemiluminescence method was used to image through the Bio-Rad gel imaging system. The quantitative value of the target protein and the corresponding internal reference protein (β-actin) was determined by Quantity One analysis software, and the ratio was the relative expression of the target protein.

Statistical analysis

Experimental data were expressed as means ± standard deviation (SD), and all calculations were performed using SPSS 22.0 statistical software. Statistical significance was evaluated using the factorial design analysis of variance. In addition, the Pearson correlation coefficients (r values) were calculated. Results were considered significant at $P<0.05$.

Results

General condition and body weight of mice in each group

The normal group and the sham group had a good diet and mental state. Their responses were rapid and their body weight increased steadily. After the bile duct ligation, the mice showed a loss in appetite, poor cognitive function, and a gradual decrease in sensitivity. Stimulation by sound and light was weakened, body hair was dull and scattered, and skin was yellow and discolored. Mice also suffered hair loss, yellow urine and feces, and gradual weight loss.

Histopathologic changes of the liver, kidney, and lung in mice

In the normal group and the sham group, the hepatic lobule was structurally intact, and the

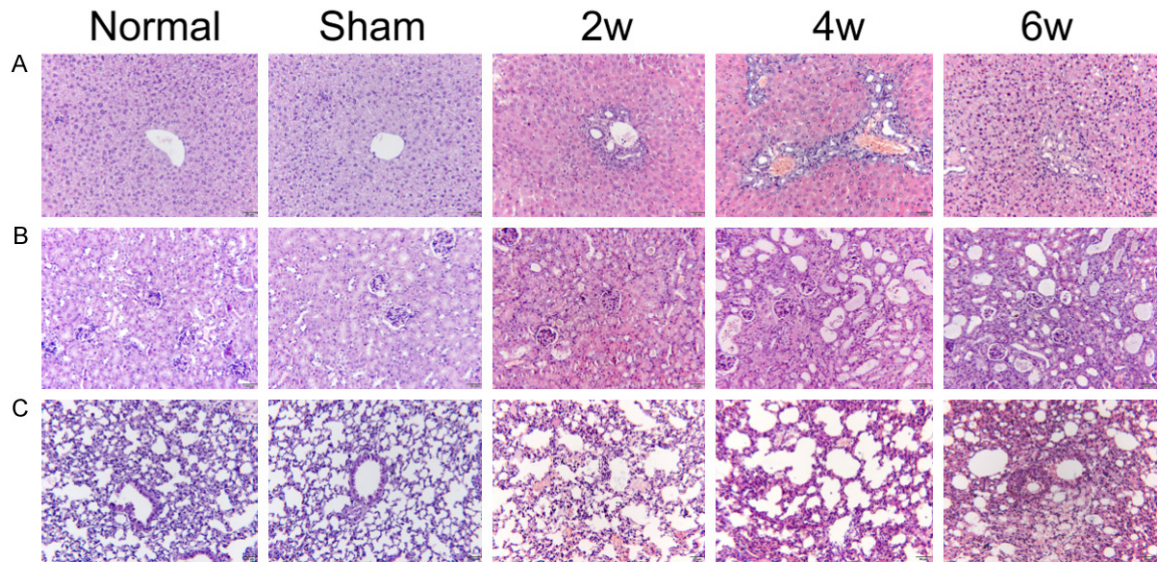

Figure 1. Histologic changes of liver, kidney and lung tissues at different time points were observed by H&E staining (original magnification ×200). A. Liver histology changes; B. Kidney histology changes; C. Lung histology changes.

hepatic cell cords were arranged neatly and radially around the central vein. The H&E staining of liver tissue in the BDL group showed that the portal area was enlarged at 2 weeks, the bile duct was dilated, and the inflammatory cells infiltrated the portal area and bile duct; at 4 weeks, the portal area gradually increased, the bile duct expanded, and a large number of hyperplastic small bile ducts and inflammatory cells infiltrated the portal area; at 6 weeks of hepatocyte arrangement disorder, marked inflammatory cell infiltration occurred, together with some hepatocyte deformation and necrosis (**Figure 1A**).

In the normal group and the sham group, epithelial cells of glomeruli and tubules were neatly arranged. There were no obvious pathologic changes in the kidneys, but only in a few connective tissues. At 2 weeks, swelling of renal cells and infiltration of inflammatory cells in the renal interstitium were observed in the BDL group; at 4 weeks, the renal tubular epithelial cells were irregularly arranged, and infiltration of the inflammatory cells in the renal interstitium increased; at 6 weeks, the renal tubular epithelial cells were unsystematically arranged. Infiltration of inflammatory cells in the interstitium, together with a marked increase of connective tissue were observed (**Figure 1B**).

In the normal group and the sham group, alveolar structure was intact, and the alveolar cavity was clear. At 2 weeks of the BDL group, some alveolar spaces and interstitial inflammation were seen, and thickening of the alveolar septum was noticed; at 4 weeks, some alveolar collapse and atelectasis were observed, accompanied by pulmonary interstitial hemorrhage and a large amount of inflammatory cell infiltration; at 6 weeks, extensive hyperemia and pulmonary vascular macrophages were observed in the lung tissue, and inflammatory cells increased (**Figure 1C**).

Distribution and expression of IGFBPrP1, NF-κB, TNF-α, and IL-6 protein in liver, kidney, and lung tissues of each group

Immunohistochemical staining showed positive staining from brown-yellow to tan particles. At different time points in liver, kidney, and lung tissues, only a small amount of IGFBPrP1, NF-κB, TNF-α, and IL-6 protein were expressed in the normal group and sham group (**Figures 2A**, **2D** and **3A**).

Dynamic changes of IGFBPrP1, NF-κB, TNF-α, and IL-6 protein expression levels in liver tissues of each group

After BDL was performed on mice, IGFBPrP1, NF-κB, TNF-α, and IL-6 proteins were mainly expressed in the portal area and in some hepatocytes at an early stage (**Figure 2A**). All indices began to increase at 2 weeks and continued to

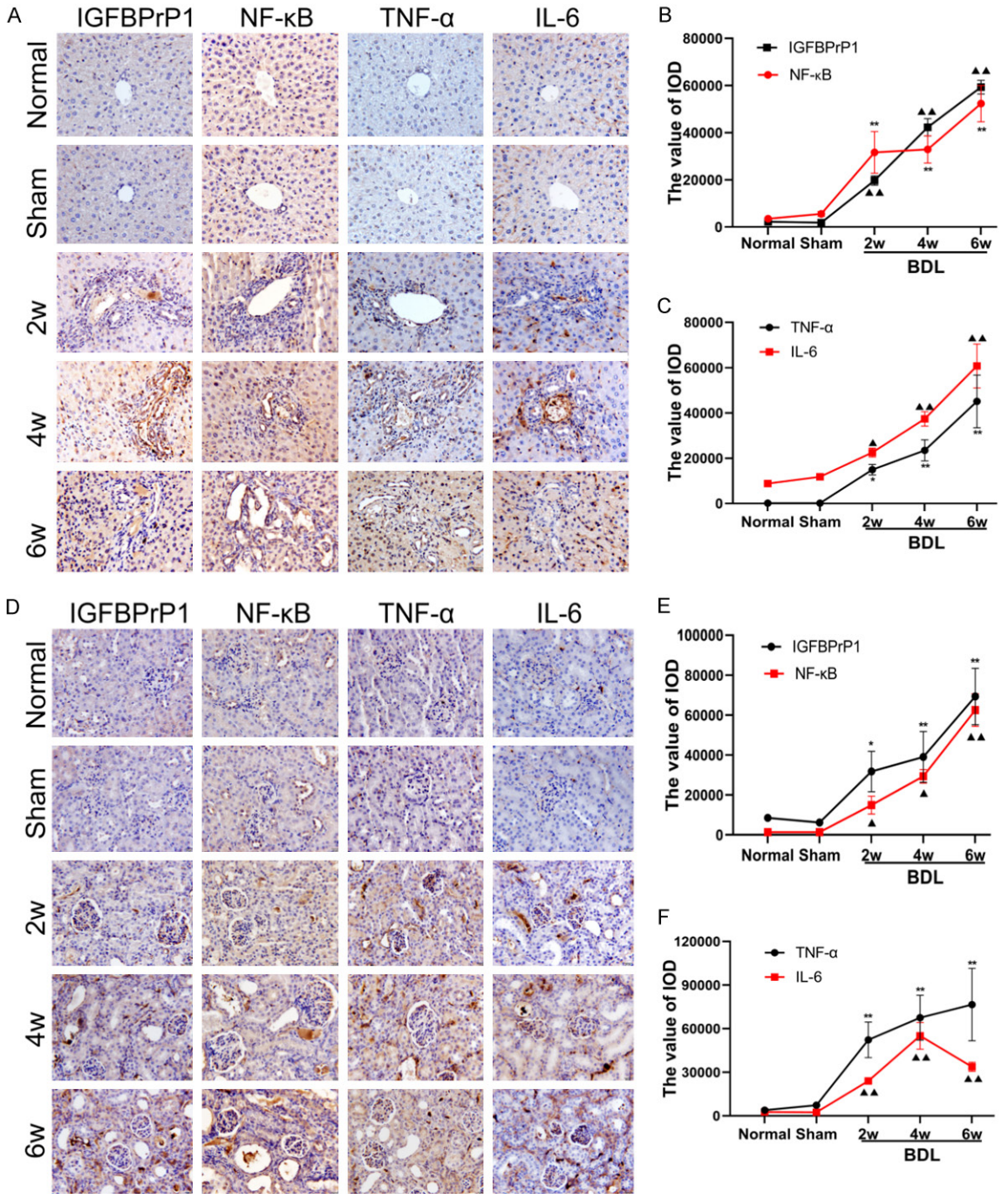

Figure 2. The expression of insulin-like growth factor binding protein-related protein 1 (IGFBPrP1), NF-κB, TNF-α, and IL-6 in liver and kidney of mice. A. Immunohistochemical staining of IGFBPrP1, NF-κB, TNF-α and IL-6 in liver tissue of mice (original magnification ×400); B and C. Dynamic changes of expression of IGFBPrP1, NF-κB, TNF-α, and IL-6 in liver tissue; D. Immunohistochemical staining of IGFBPrP1, NF-κB, TNF-α and IL-6 in kidney tissue of mice (original magnification ×400); E and F. Dynamic changes of expression of IGFBPrP1, NF-κB, TNF-α and IL-6 in kidney tissue. PBS used as a negative control. Data are presented as the mean ± SD (n=8 per group). Compared with the normal group and the sham group, ▲: $P<0.05$, ▲▲: $P<0.01$; *: $P<0.05$, **: $P<0.01$.

increase in a time-dependent manner. As the disease progressed, the expression of the above proteins increased to all hepatic lobules (**Figure 2B**, **2C**). The difference was statistically significant when compared with the normal group and the sham group ($P<0.05$).

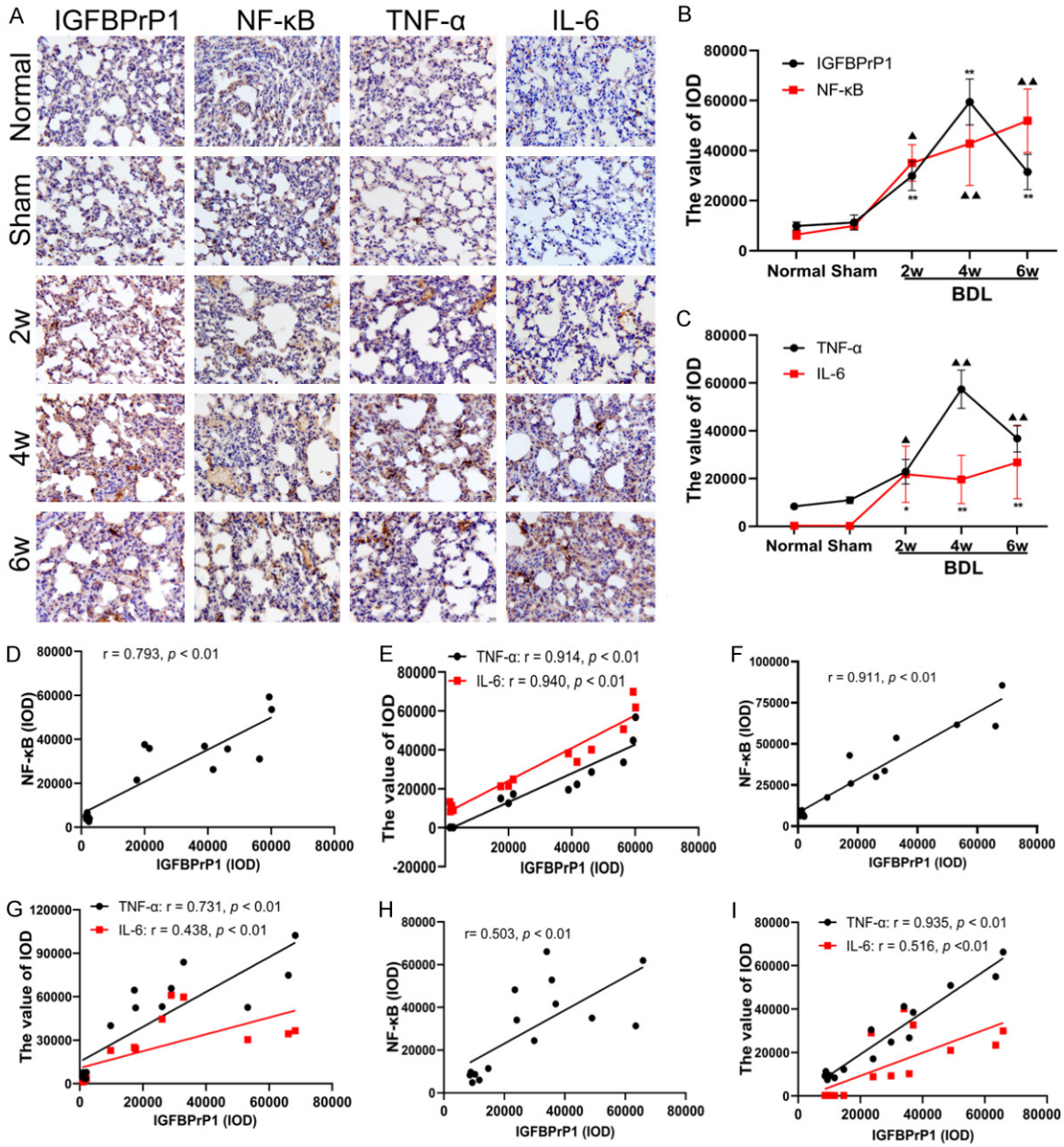

Figure 3. The expression of insulin-like growth factor binding protein-related protein 1 (IGFBPrP1), NF-κB, TNF-α, and IL-6 in lung of mice; the correlation between IGFBPrP1 and the expression of NF-κB, TNF-α and IL-6 in liver, kidney and lung tissues. A. Immunohistochemical staining of IGFBPrP1, NF-κB, TNF-α, and IL-6 in lung tissue of mice (original magnification ×400); B and C. Dynamic changes of expression of IGFBPrP1, NF-κB, TNF-α, and IL-6 in lung tissue; D and E. The correlation between IGFBPrP1 and the expression of NF-κB, TNF-α, and IL-6 in liver tissues of mice; F and G. The correlation between IGFBPrP1 and the expression of NF-κB, TNF-α and IL-6 in kidney tissues of mice; H and I. The correlation between IGFBPrP1 and the expression of NF-κB, TNF-α and IL-6 in lung tissues of mice. PBS was used as a negative control. Data are presented as the mean ± SD (n=8 per group). Compared with the normal group and the sham group, ▲: $P<0.05$, ▲▲: $P<0.01$; *: $P<0.05$, **: $P<0.01$.

Dynamic changes of IGFBPrP1, NF-κB, TNF-α, and IL-6 protein expression levels in renal tissues

After BDL was performed on mice, the four proteins were mainly expressed in renal tubular epithelial cells and renal interstitial cells (**Figure 2D**). The expression of IGFBPrP1, NF-κB, and TNF-α increased in 2 weeks in a time-dependent manner; IL-6 increased at 2 weeks, peaked at 4 weeks and slightly decreased at 6 weeks (**Figure 2E**, **2F**). When compared with

the normal group and sham group, positive expression of these proteins increased with the progression of the disease.

Dynamic changes of expression levels of IGFBPrP1, NF-κB, TNF-α, and IL-6 in lung tissue

After BDL was performed on mice, the four proteins were mainly expressed in alveolar mesenchymal cells and alveolar vascular endothelial cells (**Figure 3A**). The expression of NF-κB and IL-6 in lung tissue increased at 2 weeks in a time-dependent manner. The IGFBPrP1 and TNF-α began to increase at 2 weeks, peaked at 4 weeks and decreased slightly at 6 weeks (**Figure 3B**, **3C**). When compared with the normal group and the sham group, the positive expression of the above-mentioned proteins increased with the progression of the disease.

Correlation analysis of IGFBPrP1 with NF-κB, TNF-α, and IL-6 in liver, kidney and lung tissues

In liver tissues of mice that underwent BDL, the correlation coefficients of IGFBPrP1 with NF-κB, TNF-α, and IL-6 were r=0.793, 0.914 and 0.940, respectively (P<0.01); and displayed a positive correlation (**Figure 3D**, **3E**). In renal tissues, the correlation coefficients of IGFBPrP1 with NF-κB, TNF-α, and IL-6 were r=0.911, 0.731 and 0.438, respectively (P<0.01); and displayed a positive correlation (**Figure 3F**, **3G**). In lung tissue, the correlation coefficients of IGFBPrP1 with NF-κB, TNF-α, and IL-6 were r=0.503, 0.935 and 0.516, respectively (P<0.01); and displayed a positive correlation (**Figure 3H**, **3I**).

Protein expression levels of IGFBPrP1, NF-κB, TNF-α, and IL-6 in liver, kidney, and lung tissues

Western blot showed that the expression of IGFBPrP1, NF-κB, TNF-α, and IL-6 in the normal group and sham group were less at different time points in liver, kidney and lung tissues (**Figure 4A-I**).

After BDL was performed on mice, the expression of IGFBPrP1, NF-κB, TNF-α, and IL-6 protein in liver tissue increased with the progression of the disease at 2 weeks (**Figure 4A-C**). The expression of IGFBPrP1, NF-κB, and TNF-α protein increased at 2 weeks and continued to gradually increase with time in renal tissues; the expression of IL-6 protein increased at 2 weeks, peaked at 4 weeks, and slightly declined at 6 weeks (**Figure 4D-F**). Additionally, the expression of NF-κB and IL-6 protein in lung tissue increased at 2 weeks in a time-dependent manner; the expression of IGFBPrP1 and TNF-α protein increased at 2 weeks, peaked at 4 weeks, and decreased at 6 weeks (**Figure 4G-I**).

Discussion

Many clinical studies have shown that hepatorenal syndrome [11] and hepatopulmonary syndrome [12] are common complications in patients with liver injury. However, the pathogenesis of kidney and lung during the progression of liver injury has not been fully elucidated. In this study, we found that inflammatory cells infiltrated liver tissue, dilated small bile ducts, and disordered the arrangement of hepatocytes after BDL in mice. Pseudolobules were observed in some mice livers. Pathologic changes were aggravated gradually with extension of operation time, and this was consistent with the results of Huang et al. [8]. This indicates that inflammatory injury occurred in the liver tissue of mice after BDL. At the same time, this study also showed pathologic changes in renal and lung tissues of BDL mice, where the tubular epithelial cells were swollen, irregularly arranged, and water vacuoles disintegrated. With the extension of postoperative time, renal tubular epithelial cell necrosis, cytoplasm disintegration, and interstitial inflammatory cell infiltration occurred. Pulmonary tissue underwent extensive congestion and edema, inflammatory cell infiltration, and pulmonary capillary dilatation. With the extension of operation time, pulmonary vascular macrophages appeared and inflammatory cells increased significantly. These results suggest that inflammation of kidney and lung tissue intensified with the aggravation of liver injury after BDL in mice. In addition, the body weight of mice belonging to the BDL group was lower than that in the normal group and sham group. Overall, the general condition of these mice was worse, and may have been related to a systemic reaction after multiple organ lesions in the BDL group.

The severity of multiple organ damage caused by cholestasis is closely related to complex pro-inflammatory cytokines and inflammatory mediators. TNF-α is a major factor in inflammatory diseases and is involved in the early stages of the inflammatory response. Excess TNF-α

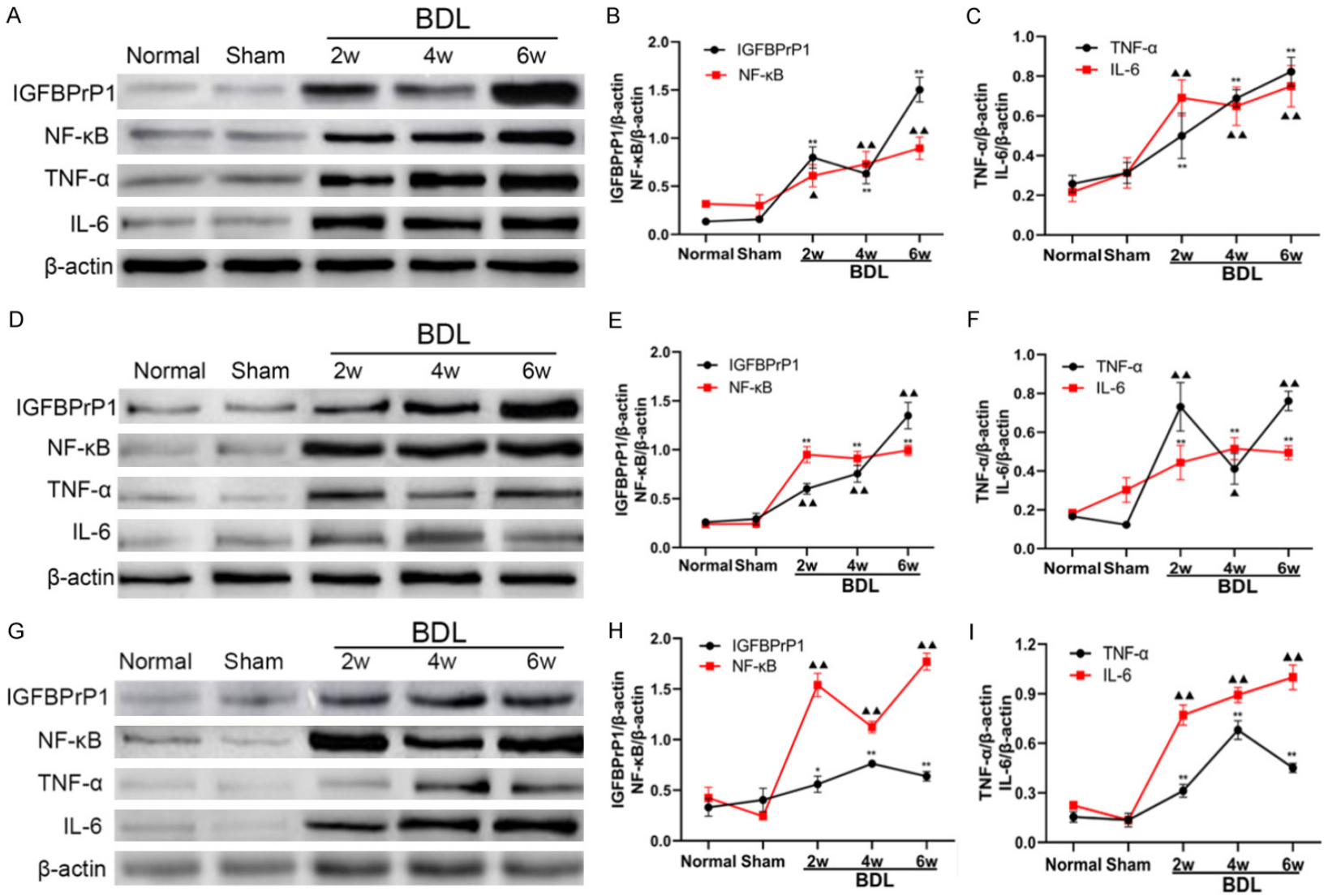

Figure 4. Western blot analysis was used to detect the expression of IGFBPrP1, NF-κB, TNF-α, and IL-6 in liver, kidney and lung tissues of mice at different time points. A-C. Expression and dynamic changes of IGFBPrP1, NF-κB, TNF-α and IL-6 in liver tissues of mice; D-F. Expression and dynamic changes of IGFBPrP1, NF-κB, TNF-α, and IL-6 in kidney tissues of mice; G-I. Expression and dynamic changes of IGFBPrP1, NF-κB, TNF-α, and IL-6 in lung tissues of mice. β-actin acted as internal control. Data are presented as the mean ± SD (n=8 per group). Compared with the normal group and sham group, ▲: $P<0.05$, ▲▲: $P<0.01$; *: $P<0.05$, **: $P<0.01$.

can induce IL-6 overexpression, and increase local endothelial cell permeability and local microcirculatory disorder, leading to an inflammation cascade, promotion of cytokine network formation, and involvement in hepatorenal syndrome [13] and hepatopulmonary syndrome [14] pathogenesis. The results show that the expression of TNF-α in liver tissue gradually increased after BDL in mice. Immunohistochemistry and western blot analysis showed that TNF-α expression in renal tissues increased at 2 weeks and continued to increase in a time-dependent manner. Studies have shown that endotoxin-induced overexpression of the cytokine TNF-α is an important mediator of high-power cycles associated with hepatorenal syndrome [15]. This also suggests a role for TNF-α in kidney damage. We speculate that after BDL in mice, local inflammation occurs in the liver tissues, and inflammatory cytokines such as TNF-α reach the kidney through blood circulation, resulting in corresponding changes in kidney tissues after liver injury. In lung tissue of mice, the expression of TNF-α in the BDL group was significantly higher than that in the normal group ($P<0.05$) and reached a peak at 4 weeks. In addition, Zhang et al. [16] found that inhibition of TNF-α reduced mononuclear/macrophage accumulation and angiogenesis in the pulmonary arteries. This shows that the pro-inflammatory cytokine TNF-α plays an important role in lung tissue damage of BDL mice.

Cytokine IL-6 is the best marker of tissue inflammation and injury. In cholestasis, it is mainly produced by monocytes and macrophages induced by TNF-α. The interaction of IL-6 and TNF-α can enhance T cell proliferation and activation of polymorphonuclear leukocytes, which aggravate the severity of tissue and organ damage and increase mortality [17]. Many studies have shown that early infection, body injury, and inflammation can lead to abnormal increase of IL-6 expression, and to organ metabolic disorders and functional damage [18]. In our study, the expression of IL-6 in liver tissues of mice after BDL showed an increasing trend that was consistent with its pathologic changes, suggesting that IL-6 may reflect the degree of liver injury. Immunohistochemistry and western blot analysis showed that the expression of IL-6 in kidney tissue of BDL group was significantly higher ($P<0.05$) than that of the normal group at each time point, reached a peak at 4 weeks and slightly decreased at 6 weeks, suggesting that the inflammation injury in kidney tissue of mice after BDL may be most severe at 4 weeks. This may later inhibit the activity of interleukins due to the accumulation of chemokines such as prostaglandin El, thereby reducing the expression level of IL-6 [19]. The expression of IL-6 in lung tissue increased with time and was significantly higher than that in the normal group ($P<0.05$), suggesting that the degree of inflammatory injury in lung tissue increased with time.

As a transcription factor, NF-κB plays a major role in inflammation and immune response, because many inflammation-related genes are regulated by NF-κB [20]. Over-activation of NF-κB can induce the overexpression of pro-inflammatory cytokines TNF-α and IL-6, thus accelerating the toxicity of multi-organ cells [21]. This study has confirmed the pro-inflammatory cytokine TNF-α and IL-6 as major target genes of NF-κB regulation and are expressed in kidney and lung tissues of cholestasis mice. This study also showed by western blot analysis, in the liver tissues of mice in the BDL group that the expression of NF-κB protein began to increase at 2 weeks and continued to increase in a time-dependent manner. The immunohistochemical staining results showed that the nucleus was markedly stained, i.e., there was activation and nuclear translocation of NF-κB, which was consistent with the results of Moczydlowska et al. [22]. The expression of NF-κB in renal and lung tissues is similar to that of liver tissue. It suggests that after BDL, when stimulated by endotoxin, cytokines, and reactive oxygen species (ROS), NF-κB can be activated in the cytoplasm of hepatocytes and Kupffer cells, resulting in the release of pro-inflammatory cytokines TNF-α and IL-6. This causes liver damage and systemic reactions, further leading to kidney and lung tissue damage.

The IGFBPrP1, also known as mac25 or IGFBP-7, is a member of the IGFBP super family. IGFBPrP1 and is widely expressed in various normal tissues (brain, lung, prostate, kidney, liver and gastrointestinal tract) [23] and peripheral blood [24, 25], and is involved in regulating cell differentiation, proliferation, necrosis and apotheosis [26, 27]. Our previous study found that IGFBPrP1 promotes NF-κB transcription and expression by activating the ERK1/2 path-

way, leading to infiltration of pro-inflammatory cytokines and activation of hepatic stellate cells to promote liver injury [28]. In this study, IGFBPrP1 protein expression in the liver tissue of BDL mice began to increase in a time-dependent manner in 2 weeks, which was consistent with our previous study [8]. We also found that the expression of IGFBPrP1 in kidney and lung tissues was basically the same as that in liver tissues, suggesting that IGFBPrP1 may aggravate the injury of kidney and lung tissues by promoting the transcription and expression of NF-κB. Furthermore, Pearson correlation analysis showed that IGFBPrP1 was positively correlated with the expression of transcription factor NF-κB, proinflammatory cytokine TNF-α, and IL-6 which responds to tissue damage in liver, kidney and lung tissues of BDL mice. The results showed that the high expression of IGFBPrP1 in multiple organs of BDL mice was accompanied by activation of NF-κB and production of pro-inflammatory cytokines.

Conclusion

This study found that liver injury induced by bile duct ligation in mice can cause kidney and lung injury, and preliminarily found that the mechanism of injury may be related to the high expression of liver injury factor IGFBPrP1, transcription factor NF-κB, proinflammatory cytokine TNF-α, and IL-6 which responds to tissue damage in kidney and lung tissues. In addition, increased expression of IGFBPrP1 may be associated with activation of the NF-κB inflammatory pathway. This provides a new strategy for the study of pathogenesis of hepatorenal syndrome and hepatopulmonary syndrome caused by cholestasis.

Acknowledgements

This study was supported by grants from National Natural Science Foundation of China (81670559); sponsored by the Fund for Shanxi Key Subjects Construction (FSKSC), sponsored by the Fund for Shanxi "1331 Project" Key Subjects Construction (1331KSC); Key Research and Development Project of Shanxi Province (201603D421023). Graduate Student Education Innovation Project of Shanxi (2019SY242; 2019BY075).

Disclosure of conflict of interest

None.

Address correspondence to: Dr. Li-Xin Liu, Experimental Center of Science and Research, The First Hospital of Shanxi Medical University, 85 Jiefang South Road, Yingze District, Taiyuan 030001, Shanxi, China. Tel: +86-351-4639039; Fax: +86-351-4639039; E-mail: lixinliu6@hotmail.com

References

[1] Zhang XP, Jiang J, Yu YP, Cheng QH and Chen B. Effect of Danshen on apoptosis and NF-kappaB protein expression of the intestinal mucosa of rats with severe acute pancreatitis or obstructive jaundice. Hepatobiliary Pancreat Dis Int 2010; 9: 537-546.

[2] Xiping Z, Chuyang L, Jie Z, Yuefang R and Meili M. Protection of Salvia miltiorrhizae to the spleen and thymus of rats with severe acute pancreatitis or obstructive jaundice. Mediators Inflamm 2009; 2009: 186136.

[3] Garcia-Tsao G, Parikh CR and Viola A. Acute kidney injury in cirrhosis. Hepatology 2008; 48: 2064-2077.

[4] Bittencourt PL, Farias AQ and Terra C. Renal failure in cirrhosis: emerging concepts. World J Hepatol 2015; 7: 2336-2343.

[5] Liu L, Mu Q, Li W, Xing W, Zhang H, Fan T, Yao H and He L. Isofraxidin protects mice from LPS challenge by inhibiting pro-inflammatory cytokines and alleviating histopathological changes. Immunobiology 2015; 220: 406-413.

[6] Mei X, Xu D, Xu S, Zheng Y and Xu S. Novel role of Zn(II)-curcumin in enhancing cell proliferation and adjusting proinflammatory cytokine-mediated oxidative damage of ethanol-induced acute gastric ulcers. Chem Biol Interact 2012; 197: 31-39.

[7] Lappas M, Permezel M, Georgiou HM and Rice GE. Nuclear factor kappa B regulation of proinflammatory cytokines in human gestational tissues in vitro. Biol Reprod 2002; 67: 668-673.

[8] Huang TJ, Ren JJ, Zhang QQ, Kong YY, Zhang HY, Guo XH, Fan HQ and Liu LX. IGFBPrP1 accelerates autophagy and activation of hepatic stellate cells via mutual regulation between H19 and PI3K/AKT/mTOR pathway. Biomed Pharmacother 2019; 116: 109034.

[9] Guo X, Zhang H, Zhang Q, Li X and Liu L. Screening for and validation of a hepatic fibrosis-related pathway induced by insulin-like growth factor-binding protein-related protein 1. Eur J Gastroenterol Hepatol 2016; 28: 762-772.

[10] Enguita M, Razquin N, Pamplona R, Quiroga J, Prieto J and Fortes P. The cirrhotic liver is depleted of docosahexaenoic acid (DHA), a key modulator of NF-kappaB and TGFbeta pathways in hepatic stellate cells. Cell Death Dis 2019; 10: 14.

[11] Belcher JM, Sanyal AJ, Peixoto AJ, Perazella MA, Lim J, Thiessen-Philbrook H, Ansari N, Coca SG, Garcia-Tsao G and Parikh CR; TRIBE-AKI Consortium. Kidney biomarkers and differential diagnosis of patients with cirrhosis and acute kidney injury. Hepatology 2014; 60: 622-632.

[12] Kawut SM, Ellenberg SS, Krowka MJ, Goldberg D, Vargas H, Koch D, Sharkoski T, Al-Naamani N, Fox A, Brown R, Levitsky J, Oh JK, Lin G, Song N, Mottram C, Doyle MF, Kaplan DE, Gupta S and Fallon MB. Sorafenib in hepatopulmonary syndrome: a randomized, double-blind, placebo-controlled trial. Liver Transpl 2019; 25: 1155-1164.

[13] Liu C, Cai J, Cheng Z, Dai X, Tao L, Zhang J and Xue D. Xiayuxue decoction reduces renal injury by promoting macrophage apoptosis in hepatic cirrhotic rats. Genet Mol Res 2015; 14: 10760-10773.

[14] Liu L, Liu N, Zhao Z, Liu J, Feng Y, Jiang H and Han D. TNF-alpha neutralization improves experimental hepatopulmonary syndrome in rats. Liver Int 2012; 32: 1018-1026.

[15] Wen Y, Wang JY and Liu P. Tumor necrosis factor-alpha enhances the effect of endothelin on renal vasoconstriction in isolated perfused rat kidney. Zhonghua Gan Zang Bing Za Zhi 2003; 11: 583-585.

[16] Zhang J, Luo B, Tang L, Wang Y, Stockard CR, Kadish I, Van Groen T, Grizzle WE, Ponnazhagan S and Fallon MB. Pulmonary angiogenesis in a rat model of hepatopulmonary syndrome. Gastroenterology 2009; 136: 1070-1080.

[17] Li W, Wang X, Niu X, Zhang H, He Z, Wang Y, Zhi W and Liu F. Protective effects of nobiletin against endotoxic shock in mice through inhibiting TNF-alpha, IL-6, and HMGB1 and regulating NF-kappaB pathway. Inflammation 2016; 39: 786-797.

[18] Lu Y, Yang Y, He X, Dong S, Wang W, Wang D and Zhang P. Esmolol reduces apoptosis and inflammation in early sepsis rats with abdominal infection. Am J Emerg Med 2017; 35: 1480-1484.

[19] Matsuura Y, Nishi S, Kariya N, Shimadzu K and Asada A. The effects of norepinephrine and prostaglandin E1 on pharmacokinetics of lidocaine in isolated perfused rat liver. Life Sci 2001; 68: 2123-2129.

[20] Chen F, Castranova V, Shi X and Demers LM. New insights into the role of nuclear factor-kappaB, a ubiquitous transcription factor in the initiation of diseases. Clin Chem 1999; 45: 7-17.

[21] Padillo FJ, Cruz A, Segura-Jiménez I, Ruiz-Rabelo J, Vázquez-Ezquerra MR, Perea-Alvarez MD, Peña J, Briceño J and Muntané J. Anti-TNF-alpha treatment and bile duct drainage restore cellular immunity and prevent tissue injury in experimental obstructive jaundice. Int J Immunopathol Pharmacol 2007; 20: 855-860.

[22] Moczydlowska J, Miltyk W, Hermanowicz A, Lebensztejn DM, Palka JA and Debek W. HIF-1 alpha as a key factor in bile duct ligation-induced liver fibrosis in rats. J Invest Surg 2017; 30: 41-46.

[23] Degeorges A, Wang F, Frierson HF Jr, Seth A and Sikes RA. Distribution of IGFBP-rP1 in normal human tissues. J Histochem Cytochem 2000; 48: 747-754.

[24] van Breevoort D, van Agtmaal EL, Dragt BS, Gebbinck JK, Dienava-Verdoold I, Kragt A, Bierings R, Horrevoets AJ, Valentijn KM, Eikenboom JC, Fernandez-Borja M, Meijer AB and Voorberg J. Proteomic screen identifies IGFBP7 as a novel component of endothelial cell-specific Weibel-Palade bodies. J Proteome Res 2012; 11: 2925-2936.

[25] Rao C, Lin SL, Ruan WJ, Wen H, Wu DJ and Deng H. High expression of IGFBP7 in fibroblasts induced by colorectal cancer cells is co-regulated by TGF-beta and Wnt signaling in a Smad2/3-Dvl2/3-dependent manner. PLoS One 2014; 9: e85340.

[26] Pen A, Durocher Y, Slinn J, Rukhlova M, Charlebois C, Stanimirovic DB and Moreno MJ. Insulin-like growth factor binding protein 7 exhibits tumor suppressive and vessel stabilization properties in U87MG and T98G glioblastoma cell lines. Cancer Biol Ther 2011; 12: 634-646.

[27] Tomimaru Y, Eguchi H, Wada H, Kobayashi S, Marubashi S, Tanemura M, Umeshita K, Kim T, Wakasa K, Doki Y, Mori M and Nagano H. IGFBP7 downregulation is associated with tumor progression and clinical outcome in hepatocellular carcinoma. Int J Cancer 2012; 130: 319-327.

[28] Guo Y, Zhang Y, Zhang Q, Guo X, Zhang H, Zheng G and Liu L. Insulin-like growth factor binding protein-related protein 1 (IGFBPrP1) contributes to liver inflammation and fibrosis via activation of the ERK1/2 pathway. Hepatol Int 2015; 9: 130-141.